Optica Applicata, Vol. LV, No. 1, 2025
DOI: 10.37190/oa/199470

Fiber optic sensing process control system based on data mining algorithm

WEI GAO

Digital Intelligence Teaching and Training Center,
The Tourism College of Changchun University,
Changchun, Jilin, 130000, China;
e-mail: gaoweinuc@sina.com

To measure the state of ethanol differentiation process, a fiber option sensing based process state monitoring system is designed. It includes a laser, demo module, PC processing module, fiber option sensing network, and state feedback control unit. A data mining algorithm for multi-parameter demo is proposed to accurately achieve temperature and strain field classification and combine accuracy to the different weights of temperature and strain on different positions, improving the correlation between wavelengths offset and state parameters. The experiment compared four common abnormal situations, The experiment adopts the method of collecting the temperature field inside the tank and the stress field outside the tank, with strain testing of 100–5000 με and temperature testing range of 0–120 °C. The results showed that the average temperature sensitivity after calibration was 0.0102 nm/°C, and the linearity was 0.9959. The average strain sensitivity is 0.499 pm/με, and the linearity is 0.9982. Feedback control has the ability to adjust state fluctuations online, and the feedback time varies for different types of anomalies. The temperature and strain wavelength deviations after correction for all four cases are less than ±1 °C and ±50 με.

Keywords: fiber optic sensing, FBG network, data mining, industrial process equipment, optimum control.

1. Introductions

Ethyl alcohol is a type of alcohol compound with the chemical formula C_2H_6O (CAS: 64-17-5). It is an important organic solvent widely used in industries such as organic synthesis [1], coating printing and dyeing [2], battery manufacturing [3], *etc*. It is also a high-performance industrial solvent with excellent solubility, and can be used as a solvent for adhesives, thinner for spray painting, *etc*. The mixed solution of ethanol and ethyl acetate is prone to form an azeotropic system, which cannot be separated and purified by general distillation methods. In order to improve the purity of ethanol distillation, precise control of temperature and pressure during the distillation process has become a key issue.

When obtaining temperature and stress information at the testing location, the detection equipment should not be affected by the chemical reaction of ethanol distillation

and should have good explosion-proof properties. Traditional detection methods are divided into contact measurement and non-contact measurement. Contact measurement is the installation of temperature sensors and piezoelectric sensors (*e.g.* platinum thermistor sensor PT100) on the ethanol distillation tank, which has high accuracy and good stability. But it can only be installed outside the tank because the sensor will corrode inside the tank. The response current generated by sensors poses certain safety hazards. Non-contact measurement uses an infrared thermal imager to obtain temperature field information of the tank body, which can complete three-dimensional temperature field reconstruction and facilitate global analysis. But it cannot obtain accurate stress changes inside the tank and cannot obtain internal temperature distribution.

Fiber optic sensing technology [4-7] uses fiber optic as a transmission medium, with small size, insulated, and distributable deployment, which has important advantages for industrial process monitoring. KHAN *et al*. [8] proposed using an improved cantilever beam combined with fiber Bragg grating (FBG) [9] to improve the accuracy of fluid acceleration testing. It has been applied to the measurement of solution flow velocity in tanks and has good stability. LIU *et al*. [10] used neural network optimization algorithms to model the microwave thermal process and discussed the control of the thermal process based on feedback parameters, with a temperature measurement accuracy of ±1 °C. XU *et al*. [11] deployed a fiber optic sensing network in the transformer tank to achieve real-time collection of the online status of the substation process, with a temperature measurement accuracy of better than 2 °C at the target location. KUANG *et al*. [12] used strain FBG to monitor the stress field of the tank structure, obtaining a strain resolution of 1.3 μm/με, which can achieve real-time monitoring of the stress field of the tank during the reaction process. LIU *et al*. [13] applied FBG network to intelligent assembly, achieving strain response detection and feedback control with a minimum of 25 με.

The existing ethanol distillation process already has some monitoring equipment, such as pressure gauges on the reactor. However, the biggest problem with traditional thermometers and pressure gauges is that they can only display the temperature or stress values obtained at the testing location, and cannot construct a complete three-dimensional temperature field or three-dimensional strain field information. So the monitoring devices on traditional equipment often only provide the problem of significant temperature or pressure exceeding the limit, which is suitable for ensuring production safety. But for this system, it can provide accurate temperature control data for the full reaction of chemical processes. It has been supplemented in the introduction section and combined with this, the research significance of this article has been presented. Using data mining algorithms to classify and process the data obtained from FBG monitoring networks, in order to achieve online monitoring and feedback control of the reaction process and achieve optimal results. The main contribution of this article is to apply data mining algorithms to industrial process monitoring and control based on fiber optic sensing networks, improving the efficiency and safety of online monitoring of ethanol distillation processes.

2. Fiber optic sensing process control system

2.1. System composition

The control system for ethanol distillation process includes computer, demodulator, controller, and FBG array, as shown in Fig. 1. FBG array collects temperature and stress information of reaction tanks and distillation tanks. The material of FBG is silicon dioxide, similar to glass, with good stability. It remains in a solid state during the ethanol distillation process and does not undergo chemical reactions with the materials inside the tank. The test signal is transmitted to the demodulator through optical fiber, and the demodulated wavelength offset data is imported into the computer. The wavelength information is used to reconstruct the temperature field distribution and stress field distribution at corresponding positions, in order to analyze whether the state during ethanol distillation is normal. By solving the model and providing corresponding processing data, closed-loop control of material input is completed.

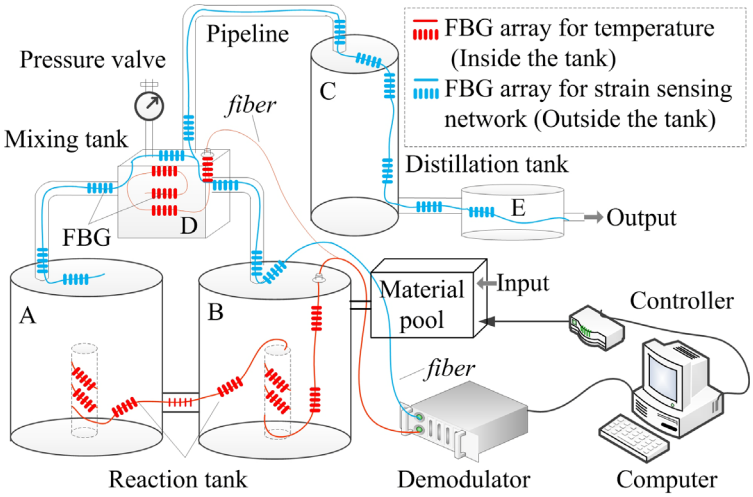

Fig. 1. Control system for ethanol distillation process based on FBG array.

During the ethanol distillation process, the system can monitor the temperature field distribution inside reaction tank A, reaction tank B, and mixing tank D. The temperature field information can be used to analyze state issues such as whether the reaction process is sufficient, thereby providing feedback on the quantity and speed of materials added to the control system. The distribution design of temperature sensitive FBG sensors mainly depends on the temperature field distribution of the chemical reaction tank. To obtain the temperature field inside the tank, the FBG sensor is fixed at the center position inside the tank, and the solution flow throughout the reaction process has little effect on it. To control the accurate temperature of ethanol distillation process in tank A and tank B, temperature sensitive FBG sensors are installed inter-

nally. In the "mixing tank", due to the occurrence of a large number of chemical reactions, temperature monitoring is required, so a temperature sensitive FBG sensor is installed. Therefore, temperature sensitive FBG arrays were installed inside reaction tanks A and B. The packaging structure of the FBG sensor is a cylindrical steel pipe, and the FBG sensitive area is cured with thermal conductive adhesive between the steel body. The purpose of this packaging is to achieve good thermal conductivity, but it is insensitive to stress, thus avoiding cross-sensitivity issues between temperature and strain. The system can monitor the pressure field distribution at the connection position and top of distillation tank C and mixing tank D. The pressure at the interface will significantly increase, so using strain sensitive FBG sensors is more suitable. So strain sensitive FBG sensors are mainly concentrated at interface positions. The pressure field information can be used to analyze whether there is deformation in the tank body and whether there is a risk of local stress imbalance. Thus, the feedback control pressure valve releases a certain pressure to ensure the safe operation of the distillation process.

Compared to traditional electric sensors, FBG arrays are made of optical fibers and are passive sensors. It is completely safe to lay inside and outside the tank. Due to the risk of explosion both inside and outside the ethanol distillation process, especially in the event of electrical leakage, the use of the FBG array in this system can significantly improve safety.

2.2. Theoretical analysis

When the fiber Bragg grating structure is subjected to temperature or stress, structural deformation causes wavelength shift [14]. Utilize this linear relationship to monitor the structural state [15]. Then the wavelength change quantity $\Delta\lambda_B$ has

$$\frac{\Delta\lambda_B}{\lambda_B} = (\alpha_f + \xi)\Delta T + (1 - p_e)\Delta\varepsilon \tag{1}$$

Among them, λ_B represents the initial center wavelength of the fiber Bragg grating, in nm; λ_f represents the coefficient of thermal expansion, which characterizes the degree to which temperature affects the variation of fiber grating spacing; ξ represents the thermal optical coefficient, which characterizes the degree to which temperature affects the refractive index of optical fibers; p_ε represents the elastic optical coefficient, which characterizes the degree of stress on the refractive index of optical fibers. Three of the coefficients can be expressed as

$$\alpha_f = \frac{1}{\lambda}\frac{d\lambda}{dT}, \quad \xi = \frac{1}{n}\frac{dn}{dT}, \quad p_e = -\frac{1}{n}\frac{dn}{d\varepsilon} \tag{2}$$

Among them, λ represents wavelength, n represents refractive index, T represents temperature, and ε represents strain. ΔT and $\Delta\varepsilon$ represent the changes in temperature and strain. When the fiber optic material is selected, the variables in Eq. (1) are only

ΔT and $\Delta\varepsilon$. Through temperature compensation and stress compensation, temperature FBG and strain FBG can be used to obtain temperature and stress test values,

$$\begin{cases} \Delta T = (\alpha_f + \xi)^{-1} \dfrac{\Delta\lambda_B}{\lambda_B} + \Delta T_{compensation} \\ \Delta\varepsilon = (1 - p_e)^{-1} \dfrac{\Delta\lambda_B}{\lambda_B} + \Delta\varepsilon_{compensation} \end{cases} \tag{3}$$

Among them, $\Delta T_{compensation}$ and $\Delta\varepsilon_{compensation}$ can be obtained through experimental calibration before testing. For the ethanol distillation process, by combining the 3D coordinate data $O(x, y, z)$ of the test tank with the temperature test data, the three-dimensional temperature field of the test area can be represented as

$$\begin{bmatrix} \Delta T_1 \\ \Delta T_2 \\ \vdots \\ \Delta T_n \end{bmatrix} \begin{bmatrix} (x_1, y_1, z_1) \\ (x_2, y_2, z_2) \\ \vdots \\ (x_n, y_n, z_n) \end{bmatrix} = \begin{bmatrix} \Delta T_1(x_1, y_1, z_1) \\ \Delta T_2(x_2, y_2, z_2) \\ \vdots \\ \Delta T_n(x_n, y_n, z_n) \end{bmatrix} \tag{4}$$

By combining the three-dimensional coordinate data $O(x, y, z)$ of the test tank with the strain test data, the three-dimensional strain field of the test area can be represented as

$$\begin{bmatrix} \Delta\varepsilon_1 \\ \Delta\varepsilon_2 \\ \vdots \\ \Delta\varepsilon_n \end{bmatrix} \begin{bmatrix} (x_1, y_1, z_1) \\ (x_2, y_2, z_2) \\ \vdots \\ (x_n, y_n, z_n) \end{bmatrix} = \begin{bmatrix} \Delta\varepsilon_1(x_1, y_1, z_1) \\ \Delta\varepsilon_2(x_2, y_2, z_2) \\ \vdots \\ \Delta\varepsilon_n(x_n, y_n, z_n) \end{bmatrix} \tag{5}$$

Finally, the temperature and strain distribution $B(\Delta T, \Delta\varepsilon)$ of the entire testing area is constructed by Eqs. (4) and (5):

$$B(\Delta T, \Delta\varepsilon) = \begin{bmatrix} \Delta T_1(x_1, y_1, z_1) & \Delta\varepsilon_1(x_1, y_1, z_1) \\ \Delta T_2(x_2, y_2, z_2) & \Delta\varepsilon_2(x_2, y_2, z_2) \\ \vdots & \vdots \\ \Delta T_n(x_n, y_n, z_n) & \Delta\varepsilon_n(x_n, y_n, z_n) \end{bmatrix} \tag{6}$$

This parameter reflects the temperature field inside any tank and the stress field at sensitive locations during the ethanol distillation process, providing technical support for achieving precise control of the ethanol distillation process.

3. Multi-parameter demodulation algorithms

The main testing parameters in the ethanol distillation process are temperature (T) and stress (ε). The system controls the reaction process based on the results of the test parameters, with the main control parameters being the flow rate of the material (S), the liquid level height inside the distillation tank (L), and the stirring speed (V). Thus, closed-loop control of ethanol distillation reaction is achieved through the testing signal of fiber optic sensing network. Using data mining techniques classify and process raw data, so that data types with the same feature state have higher recognition accuracy.

When it exceeds the threshold range, the system adjusts the control parameters based on the test results for correction. Let the temperature stability range be ($T_{\min}$, $T_{\max}$) and the pressure stability range be ($F_{\min}$, $F_{\max}$), where $T_{\min}$ and $F_{\min}$ represent the minimum values in the normal state, and $T_{\max}$ and $F_{\max}$ represent the maximum values in the normal state. When the monitoring data is below the minimum value, the system supplements materials and catalysts to increase the reaction intensity and raise the temperature. On the contrary, the system reduces the reaction intensity and temperature by restricting the material flow rate, thereby ensuring a smooth industrial production process. The system provides control methods based on the deviation between FBG position and state parameters, and performs coding analysis on FBG sensors, namely $\Delta\lambda_{T_1}$, $\Delta\lambda_{T_2}$, …, $\Delta\lambda_{T_m}$ and $\Delta\lambda_{F_1}$, $\Delta\lambda_{F_2}$, …, $\Delta\lambda_{F_m}$.

According to the relationship between test parameters and control parameters, the algorithm steps are as follows:

1) Initialize control parameters, set the number of iterations l, and collect the wavelength changes of FBG at time t, including $\Delta\lambda_{T_1}$, $\Delta\lambda_{T_2}$, …, $\Delta\lambda_{T_m}$ and $\Delta\lambda_{F_1}$, $\Delta\lambda_{F_2}$, …, $\Delta\lambda_{F_m}$. Thus, temperature and strain information at corresponding positions were obtained during the ethanol distillation process.

2) Mark the three subnodes with the highest impact weight on control parameters, namely $\Delta\lambda_1$, $\Delta\lambda_2$, $\Delta\lambda_3$, and update their corresponding weight values ρ_S, ρ_L, ρ_V. Sort the wavelength offset data at each position to calculate the position with the largest deviation in current temperature and stress of the tank. Based on the positional relationship, set the weight parameters that affect the ethanol distillation process.

3) The specific data mining algorithm used in this article is support vector machine (SVM). We consider temperature T and stress F as two independent variables, and can obtain two-dimensional coordinates (T, F) during measurement. However, according to different states, the corresponding coordinate points under different abnormal conditions will have different characteristic trends. Therefore, the maximum distance between the sets of coordinate points in two different states is the optimal classification position, that is, the hyperplane equation is constructed based on these points, $w^{\mathrm{T}}x + b = 0$. Iterate all test points to calculate the distance d:

$$d = \frac{\left| W^{\mathrm{T}} * X + b \right|}{\| W \|} \tag{7}$$

Among them, $\|W\|$ is the hyperplane norm, b is the intercept, and x is the characteristic variable. The d value is used to analyze the feedback values of different states in the ethanol distillation process, in order to screen out abnormal states from the data of normal states.

4) Due to the linear effect of temperature and stress on FBG wavelength shift within the testing range, the use of linear kernel function $T^{\mathrm{T}}F$ can achieve data classification for different states. Based on this classification, precise characterization values for controlling the ethanol distillation process can be obtained, thereby achieving optimization of the reaction process.

5) Calculate the ratio k between the weight value at that moment and the optimal weight value in the standard process;

$$k = a_1 \frac{\rho_L}{\rho_{L_{\text{best}}}} + a_2 \frac{\rho_S}{\rho_{S_{\text{best}}}} + a_3 \frac{\rho_V}{\rho_{V_{\text{best}}}}, \qquad (a_1 + a_2 + a_3 = 1) \tag{8}$$

6) Establish a fitting model with ($T_{\min}$, $T_{\max}$) and ($F_{\min}$, $F_{\max}$) as boundary conditions, and loop until k reaches the optimal value.

7) Send the current state adjustment control parameters to the control module to achieve online control of the control unit. Online control can achieve the optimization of ethanol distillation process. When controlling the change process, FBG sensors collect real-time data to achieve online adjustment of control parameters. The program flowchart is shown in Fig. 2.

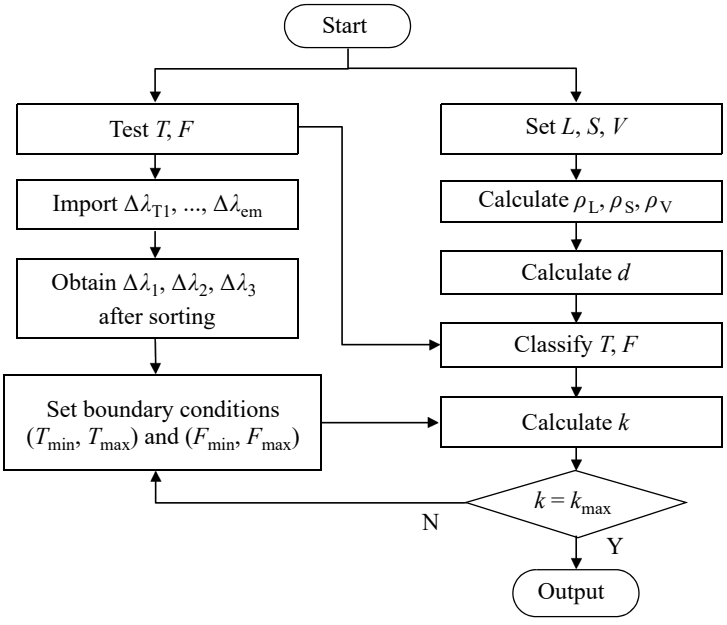

Fig. 2. Flow chart of multi-parameter demodulation algorithm based on data mining.

4. Experiments

4.1. Experimental system construction

Install two sets of FBG sensors in the ethanol distillation equipment in the laboratory to obtain temperature and stress test data, respectively. There are screw holes on both sides of the FBG temperature sensor, which are fixed inside the tank with screws. This method is very sturdy and not easy to cause detachment. FBG strain sensors is glued to the testing position, and due to the need to obtain real-time stress distribution at the testing location, using soft plastic packaging is beneficial for collecting stress fields. Because it is fixed on the outside of the tank, it will not be corroded by chemical reactions inside the tank. A multi-parameter control system based on wavelength response was established to control the ethanol distillation process online, as shown in Fig. 3. The system consists of a computer, fiber Bragg grating demodulation module, FBG sensor, and JZCS8000 (II) integrated process control device. The FBG sensor used for temperature testing is encapsulated in a cylindrical steel tube, with a length of 3 cm and a diameter of 3 mm. The FBG sensor used for stress testing adopts a deformable sheet structure with dimensions of 20 mm × 5 mm. The modulation range of the demodulation module is 1525–1565 nm, and the demodulation accuracy is ±1 pm. The system is shown in Fig. 3.

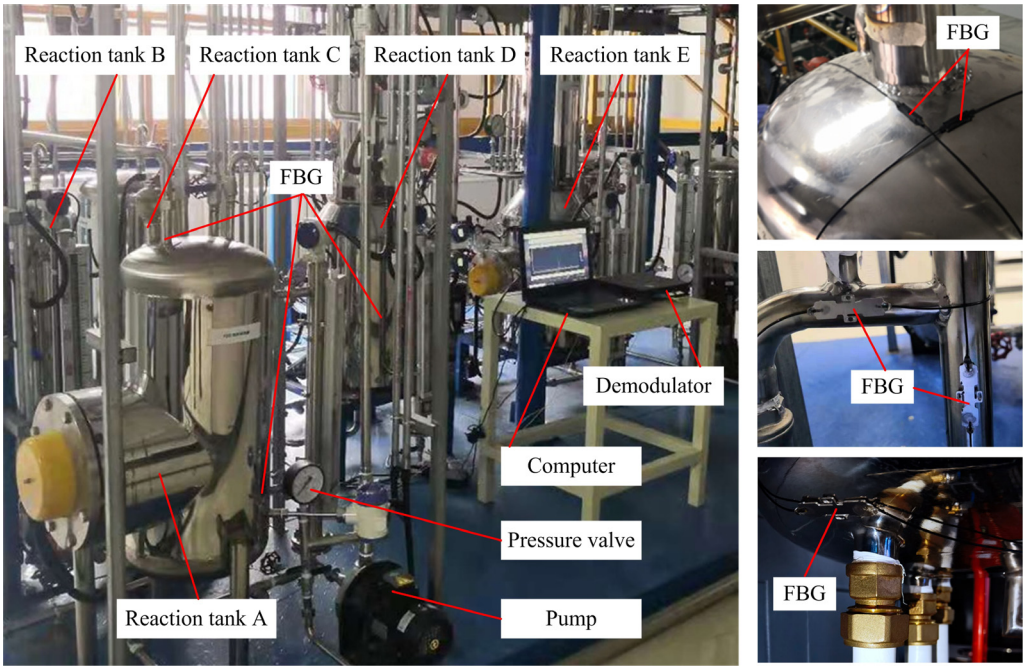

Fig. 3. Fiber optic sensing monitoring system for ethanol distillation process.

In Fig. 3, the FBG distribution is determined by the sensitivity type and degree at different positions during the ethanol distillation process. The position distribution design of FBG in Fig. 1 shows that FBG temperature sensors are mainly distributed inside the reaction tank and mixing tank to obtain temperature data, while FBG strain sensors are mainly distributed in the connecting pipe, tank interface, and tank bottom. And in order to obtain the strain direction information at these test positions, the strain FBG sensors are arranged in an orthogonal structure. The FBG temperature sensor adopts a metal encapsulated protective structure, which can ensure good thermal conductivity and prevent interference from the stress field of the tank body, achieving decoupling of temperature and strain. The FBG stress sensor adopts a plastic soft packaging structure, which is attached to each storage tank with large curvature or interface attachments, and temperature responsive FBG sensors are attached to adjacent positions to achieve stress measurement and temperature compensation.

4.2. Sensor parameter selection

The core container of the distillation process is the plate distillation tower, with a product concentration monitoring parameter measurement range of 0–20% and an accuracy of ±1%. According to the process requirements, the operating temperature should be between 78 and +120 °C, and the pressure inside the distillation tower should be between 0 and +0.3 MPa. By controlling the feed rate and stirring speed of the distillation tower, the temperature and pressure are maintained within appropriate ranges. The FBG temperature sensor used is The KS-S-FBG-ST fiber Bragg grating temperature sensor from CASSTK company, which has a temperature resolution of 0.1 °C and a size of ∅ 3 × 55 mm. The FBG temperature sensor applied inside the tank needs to be wrapped in a corrosion-resistant coating structure to enhance its stability. It adopts cylindrical steel barrel packaging The FBG strain sensor adopts MUST type FBG sensor, with dimensions of 25 × 10 × 1 mm and flexible plastic packaging. The measurement accuracy of FBG temperature sensor is ±1.5%, and the temperature measurement range is from −40 °C to +300 °C. The measurement accuracy of FBG pressure sensor is ±1.5%, and the measurement range is from −0.1 to +0.5 MPa. And FBG is a passive sensor, which is absolutely safe compared to electrical sensors. According to the above requirements, if the bandwidth of the FBG sensor is set to be less than 0.3 nm, the sidelobe suppression ratio is greater than 15 dBm, and the reflectivity is greater than 90%, the temperature and strain data of the target position can be well obtained. The sensor design parameters are shown in Table 1.

T a b l e 1. Selection of sensor parameters.

FBG type	Sensitivity	Maximum test value	3 dBm bandwidth	Interface	Insertion loss	Work temperature
Temperature	99.781 °C/nm	120 °C	≤ 0.3 nm	FC/APC	≤ 0.3 dBm	−30–120 °C
Pressure	−1.131 kPa/nm	0.3 MPa	≤ 0.3 nm	FC/APC	≤ 0.3 dBm	−30–120 °C

5. Experimental data analysis

5.1. Calibration tests for temperature and strain

In order to eliminate the cross-sensitivity between temperature and strain during the testing process, a stress insensitive FBG temperature sensor is used to obtain temperature and calibrate the test data of the FBG strain sensor. In the reactor, the structure used for FBG temperature sensors has almost no response to pressure, so it can fully reflect temperature characteristics. FBG strain sensors are simultaneously affected by temperature and pressure, so using FBG temperature sensors can calibrate the temperature offset of FBG strain sensors.

Firstly, complete the calibration test of the FBG temperature sensor by placing it in a GDW/GDJS-100 constant temperature chamber for testing. Record the test data every 5 °C. The wavelength shift between the FBG temperature sensor and the FBG strain sensor is shown in Fig. 4

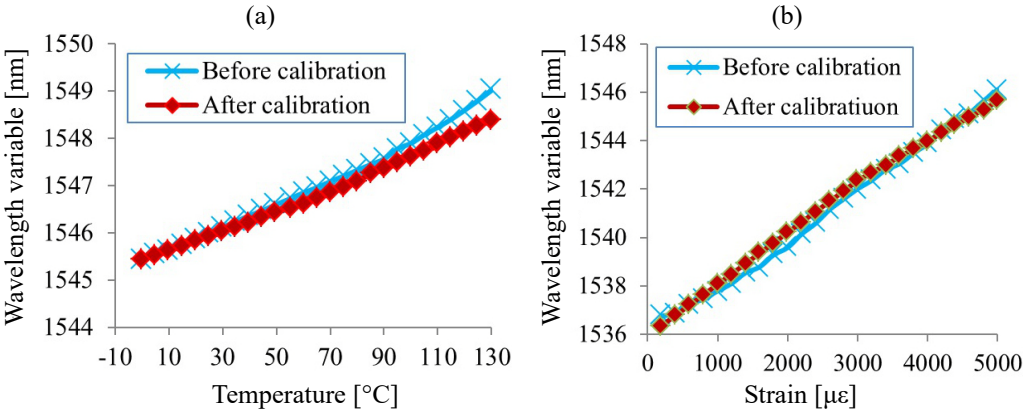

Fig. 4. Temperature and strain calibration test of FBG sensor. (a) Temperature testing calibration, and (b) strain testing calibration.

As shown in Fig. 4(a), the test data of the FBG temperature sensor before calibration shows a certain nonlinear increase in wavelength shift with the increase of temperature after 60 °C, with a linearity of 0.9923. After calibration, the slope of the temperature test data change curve was 0.0102 nm/°C, and the linearity increased to 0.9959. As shown in Fig. 4(b), there is a slight deviation in strain around 2000 με. After calibration, the average sensitivity of the strain sensing unit is 0.499 pm/με. The linearity has increased from 0.9965 to 0.9982. The use of standard temperature and strain sensors can calibrate the test data of FBG temperature sensors and FBG strain sensors, thereby improving the accuracy of test values within the testing range. And the test data from FBG temperature sensors can compensate for the temperature offset of FBG strain sensors, thereby solving the problem of cross-sensitivity between temperature and strain.

5.2. FBG networking test

Due to the stress insensitive nature of FBG temperature sensors, as long as the FBG strain sensor network can complete the inversion of the three-dimensional stress field, it can ensure that the system can obtain the main state parameter information of ethanol distillation. By networking the FBG strain sensors on the reaction tank, it is possible to analyze the strain situation at different locations based on different FBG responses. Taking the pressure changes at the connection between the middle of the tank body and the tank body as an example, wavelength shift data of FBG network is collected, and six characteristic positions of FBG are used for comparative analysis. The center wavelength shift of the FBG sensor reflection spectrum ($\Delta\lambda_B$) is directly proportional to the micro-strain produced at the measured point. The test results are shown in Fig. 5.

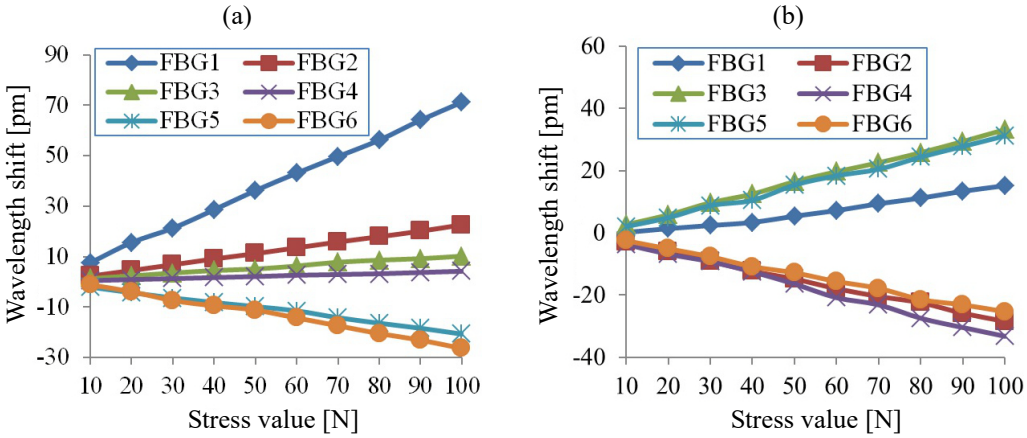

Fig. 5. Response distribution of FBG strain sensors at different stress sensitive positions. (a) Pressure in the middle of the tank, and (b) pressure at the connection port of the tank.

As shown in the test chart, when pressure is applied at different positions, the corresponding echo response has significant differences. As shown in Fig. 5(a), when stress is applied to the center position, the response of FBG1 is linear with a slope of 0.723 pm/N. Analysis suggests that this is due to the adhesive position of FBG1 being near the center point. The slope of FBG2-FBG6 varies between 0.161 and 0.223 pm/N. As shown in Fig. 5(b), when stress is applied to the interface of the tank body, FBG3 and FBG5 show a positive change with an average slope of 0.325 pm/N, while FBG2, FBG4, and FBG6 show a negative change with an average slope of −0.279 pm/N. One side of the tank interface is in a compressed state, while the other side is in a stretched state. Comparing the two graphs, it can be seen that when the stress field at different positions changes differently, the FBG response echo at different positions will undergo completely different changes. This means that different echo response characteristics can be used to invert the strain state at different positions of the tank body, thereby analyzing whether the state of the reaction process is normal. From this, the strain dis-

tribution of the tank can be analyzed based on the FBG number, thereby inverting the three-dimensional stress field and providing a basis for the analysis of the ethanol distillation reaction state. For example, when FBG1 increases, it indicates an increase in pressure in the middle of the tank. If FBG2 changes from positive to negative, it indicates that the reaction rate inside the tank is too fast. And the change in raw material supply is not significant, indicating the need to adjust the supply of catalyst.

5.3. Feedback control of abnormal states during distillation process

In order to test the feedback control performance of the fiber optic sensing network for abnormal states in the distillation process, several abnormal states were artificially added to the reaction tank, and the test results and feedback control effect were observed. Four typical abnormal states were simulated and tested. Situation A: the liquid level in the reaction tank is too high. Situation B: the amount of catalyst in the catalytic batching box is too large. Situation C: the flow velocity inside the transmission pipe is too fast. Situation D: insufficient stirring in the reaction tank. All four abnormal parameters use ± 30% of the normal standard value as the initial state parameter value. The test results are shown in Table 2 by taking the average of the three most sensitive FBG sensors under each state condition.

T a b l e 2. Test results of temperature and strain over time under four different conditions.

Situation		Real-time test temperature [°C]							
		0 min	5 min	10 min	15 min	20 min	25 min	30 min	35 min
A	T [°C]	76.2	75.4	69.4	65.6	61.2	56.8	58.7	58.4
	ε [με]	1951	1879	1631	1587	1535	1472	1518	1524
B	T [°C]	98.8	92.4	85.6	86.8	86.4	86.2	86.4	86.3
	ε [με]	4478	3949	3389	3481	3468	3462	3449	3442
C	T [°C]	34.2	47.9	48.2	48.6	48.4	48.1	48.2	48.2
	ε [με]	672	944	951	957	949	953	954	951
D	T [°C]	52.7	58.6	68.8	75.4	76.3	75.4	75.7	76.2
	ε [με]	1784	1951	2372	2513	2574	2540	2532	2546

In case A, excessive material inside the main tank may result in exceeding the rated reaction capacity, so an initial temperature setting 30% higher than the standard temperature is used for simulation. After the temperature sensing FBG collects and transmits the internal temperature of the tank to the control unit, the system control input reduces the input amount. When the material consumption in the main tank is about 25 minutes, the temperature basically returns to normal. After the input quantity is restored, the temperature fluctuation remains within ±0.5 °C. The trend of strain fluctuation is basically consistent with the temperature change, with an error within ±50 με. In case B, simulate the heating phenomenon of the catalytic batching box caused by the improvement of catalytic efficiency with a 30% heat release increment. As feedback control can timely reduce the ratio after the test temperature exceeds the threshold,

the box temperature can be restored to normal in only about 10 minutes. The strain fluctuation error is within ±20 με. In case C, if the insufficient reaction caused by the rapid flow rate is simulated by reducing the temperature, the temperature sensing FBG test data at the pipeline position will control the flow rate valve to slow down. This process can basically make the process temperature reach the normal value and tend to stabilize within 5 minutes of controlling the speed, with temperature and strain errors within ±0.5 °C and ±10 °C. In case D, reducing the temperature to simulate the uneven mixing of reactants caused by insufficient stirring will accelerate the stirring process through feedback control. After about 15 minutes, the temperature and strain errors will be eliminated by the feedback, and the errors will be within ±0.8 °C and ±35 °C. By comparing the testing and feedback control results of the four scenarios comprehensively, it can be seen that the feedback time for different process anomalies has significant differences, which also verifies the feasibility of using different FBG position test data for state anomaly encoding control.

6. Conclusions

This article proposes a fiber optic sensing network system for controlling the ethanol distillation process. The system simultaneously obtains the temperature and strain field of the tank through combined measurement and differential calibration, achieving real -time monitoring and feedback control of state parameters. The experiment completed temperature testing calibration and strain testing calibration separately, and the testing accuracy was well calibrated. At the same time, simulation tests were conducted on four common abnormal states, and the results showed that temperature and strain anomalies caused by different states can be effectively identified, and feedback control can restore them to normal states within a certain period of time. After feedback control, the temperature and strain at the testing location can be restored to within 30% of the standard deviation, which meets the design requirements.

The main contribution of this article is the application of passive FBG sensing network to online monitoring of ethanol distillation process. The decoupling of temperature and strain is achieved through combined measurement and differential calibration, providing new ideas for real-time online monitoring and feedback control of ethanol distillation process.

However, as of now, this article has mainly completed the testing and feedback control of single state anomalies, and there are often more complex situations in the actual ethanol distillation process. For example, if two or more abnormal states occur simultaneously, it can lead to data aliasing in the testing data of fiber optic sensing networks. This is also a direction we plan to continue testing and improving in the future.

Acknowledgment

This work was supported by the Jilin Province Science and Technology Development Plan Project (Key R&D Project in the Field of Medicine and Health) (20220204106YY); Jilin Provincial Natural Science Foundation (20240101226JC); Jilin Provincial Department of Education Science and Technology Research Planning Project (JJKH20230815KJ); the National Science Foundation of Chinese (61703056).

References

[1] MESQUITA E., PEREIRA L., THEODOSIOU A., ALBERTO N., MELO J., MARQUES C., KALLI K., ANDRÉ P., VARUM H., ANTUNES P., *Optical sensors for bond-slip characterization and monitoring of RC structures*, Sensors and Actuators A: Physical **280**, 2018: 332-339. https://doi.org/10.1016/j.sna.2018.07.042

[2] BOTSIS J., HUMBERT L., COLPO F., GIACCARI P., *Embedded fiber Bragg grating sensor for internal strain measurements in polymeric materials*, Optics and Lasers in Engineering **43**(3-5), 2005: 491-510. https://doi.org/10.1016/j.optlaseng.2004.04.009

[3] XU O., LU S., FENG S., JIAN S., *Novel fiber-laser-based fiber Bragg grating strain sensor with high-birefringence Sagnac fiber loop mirror*, Chinese Optics Letters **6**(11), 2008: 818-820.

[4] OSÓRIO J.H., CHESINI G., SERRÃO V.A., FRANCO M.A.R., CORDEIRO C.M.B., *Simplifying the design of microstructured optical fibre pressure sensors*, Scientific Reports **7**, 2017: 2990. https://doi.org/10.1038/s41598-017-03206-w

[5] WANG G.N., ZENG J., MU H., LIANG D.K., *Optimization of fiber Bragg gratting sensor network*, Laser & Infrared, Issue 1, 2015: 66-69.

[6] WU W., LIU X., *The application of improved genetic algorithm in fiber Bragg grating (FBG) sensor network*, [In] *2008 Second International Conference on Genetic and Evolutionary Computing*, Jinzhou, China, 2008: 3-6. https://doi.org/10.1109/WGEC.2008.88

[7] WANG Y.B., FAN X.Y., ZHANG L.L., LU G.W., YAO Y., ZHANG Z.C., *The application genetic and simulated annealing algorithm in FBG sensor network*, [In] *2008 4th International Conference on Wireless Communications, Networking and Mobile Computing*, Dalian, China, 2008: 1-4. https://doi.org/10.1109/WiCom.2008.3024

[8] KHAN M.M., PANWAR N., DHAWAN R., *Modified cantilever beam shaped FBG based accelerometer with self temperature compensation*, Sensors and Actuators A: Physical **205**, 2014: 79-85. https://doi.org/10.1016/j.sna.2013.10.027

[9] DU Y., SUN B., LI J., ZHANG W., *Fiber Bragg grating sensor*, [In] *Optical Fiber Sensing and Structural Health Monitoring Technology*, Springer, Singapore, 2019: 77-148. https://doi.org/10.1007/978-981-13-2865-7_3

[10] LIU T., LIANG S., XIONG Q., WANG K., *Integrated CS optimization and OLS for recurrent neural network in modeling microwave thermal process*, Neural Computing and Applications **32**, 2020: 12267-12280. https://doi.org/10.1007/s00521-019-04300-y

[11] XU Z., ZHANG S., LIAO H., *et al*., *Integrated technology of distributed optical fiber and transformer electromagnetic wire*, Proceedings of the CSEE **41**(19), 2021: 6816-6826.

[12] KUANG Y., GUO Y., XIONG L., LIU W., *Packaging and temperature compensation of fiber Bragg grating for strain sensing: A survey*, Photonic Sensors **8**, 2018: 320-331. https://doi.org/10.1007/s13320-018-0504-y

[13] LIU Z.C., YANG J.H., ZHANG L., WANG G., *Granary temperature measurement network based on chirped FBG*, Guang Pu Xue Yu Guang Pu Fen Xi (Spectroscopy and Spectral Analysis) **36**(10), 2016: 3377-3380 (in Chinese).

[14] MULLE M., YUDHANTO A., LUBINEAU G., YALDIZ R., SCHIJVE W., VERGHESE N., *Internal strain assessment using FBGs in a thermoplastic composite subjected to quasi-static indentation and low-velocity impact*, Composite Structures **215**, 2019: 305-316. https://doi.org/10.1016/j.compstruct.2019.02.085

[15] YU C.W., LEI S.C., CHEN W.S., SONG S.R., *Downhole fiber optic temperature-pressure innovative measuring system used in Sanshing geothermal test site*, Geothermics **74**, 2018: 190-196. https://doi.org/10.1016/j.geothermics.2018.03.005

Received November 13, 2024
in revised form December 10, 2024